

Temperature Dependence of the NO₃ Absorption Spectrum

R. J. Yokelson,[†] James B. Burkholder,* R. W. Fox,[‡] Ranajit K. Talukdar, and A. R. Ravishankara[§]

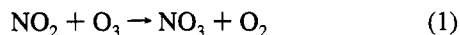
Aeronomy Laboratory, NOAA, 325 Broadway, Boulder, Colorado 80303, and The Cooperative Institute for Research in Environmental Sciences, University of Colorado, Boulder, Colorado 80309

Received: July 25, 1994; In Final Form: October 5, 1994[⊗]

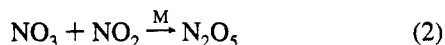
The temperature dependence of the NO₃ absorption spectrum was measured over the wavelength range 440–720 nm and temperature range 298–200 K using a diode array spectrometer. The NO₃ absorption cross section at 662 nm, the peak of the 0–0 transition, was measured using time resolved tunable diode laser absorption following 351 nm laser photolysis of a Cl₂/ClONO₂ mixture. The NO₃ absorption cross section at 662 nm was $(2.23 \pm 0.22) \times 10^{-17}$ cm² at 298 K and increased 36% in going from 298 to 200 K (2σ error limits including estimated systematic errors). These results are quantitatively compared with previous measurements.

Introduction

The nitrate free radical, NO₃, is an important species in the atmosphere and is formed primarily by the reaction of NO₂ with O₃:



In the stratosphere, NO₃ formation followed by photodissociation to NO and O₂ is a catalytic ozone removal process. In the troposphere, NO₃ is an important oxidizer during the nighttime and contributes as much as or more than the OH radical toward the removal of species such as olefins, sulfur compounds, and carbonyls. In both the stratosphere and troposphere, NO₃ converts NO_x (NO + NO₂ + NO₃) to N₂O₅ (and HNO₃) via the reaction



N₂O₅ formed in this process may be removed via heterogeneous reactions on particles producing HNO₃. The formation of HNO₃ augments the conversion of NO₂ to HNO₃ via reaction with OH and could serve as a small net source of OH upon its photolysis. Therefore, knowledge of the atmospheric chemistry of the NO₃ free radical is of interest.

NO₃ absorbs very strongly in the visible with its 0–0 band centered at 662 nm. NO₃ has been measured in the atmosphere using visible absorption techniques to infer levels of nitrogen oxides in the stratosphere and mesosphere¹ as well as the troposphere.^{2–6} Further, because NO₃ absorbs strongly in the visible, it is essentially nonexistent during daytime. The NO₃ atmospheric removal rate is governed by its photolysis rate, which depends on its absorption cross sections, quantum yields, and the solar flux. Laboratory studies also use absorption techniques to monitor NO₃ for measuring reaction rate coefficients and product yields in reactions that involve the NO₃ radical.⁷ Therefore, accurate values for the NO₃ absorption cross sections, particularly at 662 nm, and their variation with

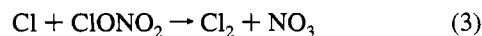
temperature are of use for laboratory studies, field measurements, and atmospheric photolysis rate calculations.

The absorption spectrum of NO₃ has been studied for many decades. For a review of previous measurements see references cited by Wayne et al.⁷ and Cantrell et al.⁸ There is reasonable agreement on the absorption cross section values at 298 K; the recent measurements agree to within 20% on the value of the cross section at 662 nm.⁷ The temperature dependence of the NO₃ radical absorption spectrum has been measured most recently by Sander,⁹ Ravishankara and Mauldin,¹⁰ and Cantrell et al.⁸ There is a significant disagreement over the temperature dependence of the absorption cross section at 662 nm. While Cantrell et al.⁸ concluded that the NO₃ absorption spectrum was invariant with temperature between 215 and 348 K, within their ±18% precision of measurements, the studies of Sander and of Ravishankara and Mauldin show an increase with decreasing temperature. Although the last two studies do not agree in the magnitude of the changes in absorption cross section with temperature, both show a systematic increase in the 0–0 transition peak cross section with decreasing temperature. Sander reports an 18% increase in going from 298 to 230 K while Ravishankara and Mauldin report a 42% increase in going from 298 to 220 K. From the above comparisons, it is clear that a remeasurement of the temperature dependence of the absorption cross sections of NO₃ is warranted.

In addition to the above reasons, we required absolute cross section values for NO₃ as a function of temperature in the course of our recent studies of the quantum yield for NO₃ production in ClONO₂ photolysis.¹¹ Therefore, we measured the NO₃ absorption cross sections over the temperature range 298–200 K. In this paper, we describe these measurements and compare our temperature dependent absorption cross sections with those from previous studies.

Experimental Details

In this study three separate sets of measurements were carried out. First, the NO₃ absolute absorption cross section at 662 nm was measured as a function of temperature using pulsed photolysis with time-resolved tunable diode laser absorption of NO₃. NO₃ was produced from the reaction



following laser photolysis of Cl₂ in the presence of ClONO₂. Next, the absorption spectrum over the wavelength range 440–

[†] Present address: Department of Chemistry, University of Montana, Missoula, MT 59812.

* To whom correspondence should be sent at: NOAA R/E/AL2, 325 Broadway, Boulder, CO 80303.

[‡] National Institute of Standards and Technology, Time and Frequency Division, 325 Broadway, Boulder CO 80303.

[§] Also affiliated with the Department of Chemistry and Biochemistry, University of Colorado, Boulder, CO 80309.

[⊗] Abstract published in *Advance ACS Abstracts*, November 15, 1994.

720 nm was measured using a diode array spectrometer in conjunction with a low-pressure discharge flow apparatus. These spectra were converted to absolute cross sections using the absolute cross sections measured at 662 nm. Last, a few measurements were carried out in a discharge flow apparatus equipped with two absorption cells in series, one at 298 K and the other at 220 K. These measurements were made to semiquantitatively measure the changes in cross sections as a function of temperature. Because NO₃ was generated in some experiments via reaction 3, our studies also provided rate coefficient data for this reaction at all the temperatures at which the cross sections were measured. These rate coefficient data are presented in a separate publication,¹² which also includes k_3 measured by monitoring the loss of Cl atoms.

The experimental details of the laser photolysis and diode array apparatus have been described in detail by Yokelson et al.¹¹ and Burkholder et al.,¹³ respectively, and are only briefly described below. The three types of measurements are described separately below.

Transient Absorption Measurements. The apparatus consists of four basic components: (1) a single-pass absorption cell with an optical path length of 91 cm, (2) a pulsed XeF (351 nm) excimer laser as the photolysis light source, (3) a tunable visible diode laser, and (4) a detector for measuring the intensity of the tunable visible diode laser. The concentrations of ClONO₂, O₃, and Cl₂ flowing through the absorption cell were measured using a continuous-wave deuterium lamp beam which was passed through the absorption cell and detected by a 0.28 m spectrograph equipped with a diode array detector.

The jacketed absorption cell was made of 30-mm-i.d. Pyrex tubing. The temperature was regulated by circulating methanol from a temperature-controlled bath through the jacket. Quartz windows were mounted inside the temperature controlled region and purged externally with dried N₂. For measurements at 200 K, a dual-window arrangement, where the windows are separated by an evacuated volume, was used. These window configurations minimized condensation of water vapor on the cell windows and ensured a uniform temperature over the entire optical path. Prevention of condensation in the optical path was essential for precise absorption measurements.

The laser photolysis beam and the probe beams were copropagated along the length of the absorption cell. A 10-cm-long cell containing Cl₂, in the range 10–50 Torr, was placed in the excimer laser beam path to attenuate the laser fluence to the desired value. Also, the excimer laser beam was coupled into the absorption cell with a 308 nm dichroic mirror so that only 20% of the fluence passed through the absorption cell. The output of the XeF laser consists of two equally intense sets of four lines centered at ~351.3 and ~353.7 nm. The fluence-weighted average of the laser output is at 352.5 nm and was taken to be the photolysis wavelength.

Only one absorption probe beam (diode laser or D₂ lamp) was passed through the absorption cell at a time. Mirrors, on positive position mounts, allowed quick and reproducible switching between the broad-band D₂ and single-wavelength diode laser probe beams. Mirrors were also used for switching the probe beam passing through the absorption cell into either a monochromator, a spectrograph, or photodiode for detection. The D₂ beam was directed into either the monochromator or the spectrograph, while the tunable diode laser beam was detected by a photodiode.

The diode laser, with a nominal wavelength of 662 nm, ran single mode with an output power between 0.5 and 2 mW. This beam was used to measure NO₃ transient absorption signals. The exact wavelength of the diode laser was measured using the diode array detector with a 10 μm entrance slit, which

resulted in a ~0.1 nm resolution. Lines from a Ne lamp were used to calibrate the spectrometer. The laser wavelength was stabilized at the peak of the NO₃ absorption feature, 661.9 nm, by regulating the laser current (~40 mA) and temperature (~275 K).

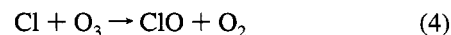
The diode laser intensity was stable to about five parts in 10⁵ on the <20 ms time scale and 200 kHz detector bandwidth used in our absorption measurements. A stable constant current was fed into the detector amplifier to offset the nominal photocurrent and a second amplification stage was used to amplify the resultant transient signals from the zeroed level. This arrangement enabled absorption measurements to be made that were limited only by the inherent amplitude noise of the diode laser. Our NO₃ detection limit was ~2 × 10¹⁰ molecules cm⁻³ for a single shot.

The monochromator/PMT system was used to measure transient UV absorption signals in the laser fluence calibration measurements and has been described in detail previously.¹³ All monochromator measurements were made using 250 μm slits, which resulted in a nominal 1.6 nm resolution. The signals from both the diode laser detector and the PMT detection systems were sent to a multichannel analyzer for digitization and signal averaging. Data acquisition was initiated approximately 1 ms before the excimer laser fired to provide a baseline signal from which the change in absorbance could be calculated. Signals were recorded at intervals in the range 5–150 μs for 1024 channels. Transient absorption profiles were measured in 10–100 coadded shots.

The procedure for measuring the absolute cross sections at 662 nm was as follows. First, the concentrations of Cl₂ and O₃ flowing through the cell were measured using the diode array spectrometer. Second, the laser fluence passing through the cell was determined by photolyzing Cl₂ at 352.5 nm in the presence of O₃ and measuring the change in absorption at 253.7 nm using the monochromator/PMT system. These constituted the actinometry experiments. Third, O₃ was replaced by ClONO₂ while keeping the Cl₂ concentration constant. Cl₂ was again photolyzed by the same laser fluence at 352.5 nm to generate Cl atoms and subsequently NO₃ via reaction 3. Finally, the concentration of ClONO₂ and Cl₂ flowing through the cell were determined by diode array measurements.

The O₃ absorption cross section at 352.5 nm (weighted average wavelength of the XeF laser) is <10⁻²² cm². The ratio of the Cl₂ to O₃ absorption cross sections at this wavelength is >1.8 × 10³, while typical concentration ratios of Cl₂ to O₃ were ~100. Hence, the amounts of ozone photolyzed and any O atoms produced were negligible compared to the amounts of Cl₂ photolyzed and Cl atoms produced. Similarly, the fraction of ClONO₂ photolyzed and its photoproducts formed were also negligible. Thus, the concentration of NO₃ produced was accurately reflected by that of Cl atoms from the photolysis of Cl₂.

The amounts of Cl₂ photolyzed could not be measured directly with the required accuracy because of the small absorption cross section of Cl₂. Therefore, ozone was added to the absorption cell to convert Cl to ClO and in the process destroy an equivalent amount of O₃ via the reaction



ClO formed in this reaction also absorbs at 253.7 nm. However, the change in the absorption at 253.7 nm was easily measurable even though the absorption by the formation of ClO partially offsets the decrease in absorption due to the loss of O₃. Assuming that one ClO is formed for each O₃ that is removed, the change in absorption measured upon photolysis of this Cl₂/O₃ mixture can be related to the number of Cl atoms produced.

It is imperative that there be no other significant sources of Cl atoms or loss of O₃. That is the reason for making the ratio of Cl₂ to O₃ or ClONO₂ as large as possible.

The laser fluence, F_{λ} , can be calculated from the measured concentrations in the absorption cell and the transient absorption signal:

$$F_{352.5} = [\text{Cl}]/(2[\text{Cl}_2]_0\sigma_{352.5}^{\text{Cl}_2}) \quad (\text{I})$$

The concentration of Cl atoms produced can be calculated from the known difference between the absorption cross sections of O₃ and ClO and 253.7 nm, which has been previously measured in our laboratory,¹⁴ and the measured change in absorption at 253.7 nm. The concentration of Cl₂ is given by the absorption measured at 330 nm using the diode array spectrometer. Thus all the needed quantities can be expressed as absorbances and cross sections to yield

$$F_{352.5} = \frac{\sigma_{330}^{\text{Cl}_2}}{2\sigma_{352.5}^{\text{Cl}_2}} \frac{1}{(\sigma_{253.7}^{\text{O}_3} - \sigma_{253.7}^{\text{ClO}})} \frac{\Delta A_{253.7}}{A_{330}} \quad (\text{II})$$

where $\Delta A_{253.7}$ is the measured change in absorbance at 253.7 nm at time t_0 , the time of the laser pulse, A_{330} is the absorbance used to determine the initial concentration of Cl₂, and $\sigma_{\lambda}^{\text{X}}$ is the absorption cross section at wavelength λ of molecule X, i.e., Cl₂, O₃, or ClO. The value of the difference in the O₃ and ClO absorption cross sections at 253.7 nm is 7.56×10^{-18} cm² independent of temperature.¹⁴

The above equation can be reduced to

$$F_{352.5} = \text{constant} \times \Delta A_{253.7}/A_{330} \quad (\text{III})$$

where the constant includes all the cross sections, which are taken from the literature. The advantage of this expression is that we are taking the ratio of absorption cross sections for Cl₂ at two wavelengths that are close to each other and a difference in absorption cross section, which was actually measured in the laboratory. The ratio of the cross sections from a given study will be more accurate than the absolute values of the cross sections, because the systematic errors in such measurements are likely to be the same and should cancel in the ratio.

In experiments with ClONO₂, where NO₃ is produced, it is necessary to add a sufficient amount of ClONO₂ and use low enough photolysis laser powers to prevent loss of Cl atoms through the reaction



where k_5 is 2.6×10^{-11} cm³ molecule⁻¹ s⁻¹.¹⁵ The effect of this reaction will be illustrated in the Results and Discussion section. The measured maximum in the transient absorbance at 662 nm is related to the concentration of the NO₃ produced and its absorption cross section:

$$\Delta A_{662} = [\text{NO}_3]l\sigma_{662}^{\text{NO}_3} \quad (\text{IV})$$

where l is the path length. Since the concentration of NO₃ produced is taken to be equal to the initial amount of Cl atoms, the above equation can be rewritten as

$$\Delta A_{662} = [\text{Cl}]l\sigma_{662}^{\text{NO}_3} = 2[\text{Cl}_2]F_{352.5}\sigma_{352.5}^{\text{Cl}_2}l\sigma_{662}^{\text{NO}_3} \quad (\text{V})$$

Combining this equation with expression III for fluence yields

$$\sigma_{662}^{\text{NO}_3} = (\sigma_{253.7}^{\text{O}_3} - \sigma_{253.7}^{\text{ClO}}) \frac{\Delta A_{662}}{\Delta A_{253.7}} \quad (\text{VI})$$

The NO₃ absorption cross section depends only on the measured changes in the absorptions and the known (previously measured) difference in absorption cross sections. Therefore, all experiments were carried out in back-to-back measurements (fluence and NO₃) while maintaining a constant concentration of Cl₂. In this way all terms related to [Cl] (Cl₂ photodissociation quantum yield, optical path length, and absorption cross section of Cl₂ at the photolysis wavelength) cancel, which eliminates many potential sources of uncertainty. The quantity $(\sigma_{253.7}^{\text{O}_3} - \sigma_{253.7}^{\text{ClO}})$ has been directly measured in previous experiments¹⁴ to be $(7.56 \pm 0.45) \times 10^{-18}$ cm² (2σ error limit). The uncertainty in this value will directly contribute to the uncertainty of our NO₃ absorption cross sections. However, $(\sigma_{253.7}^{\text{O}_3} - \sigma_{253.7}^{\text{ClO}})$ is temperature independent, and therefore uncertainty in its value does not influence our measured temperature dependence of the NO₃ absorption cross sections. Our quoted uncertainty in $\sigma_{662}^{\text{NO}_3}$ includes the uncertainty in $(\sigma_{253.7}^{\text{O}_3} - \sigma_{253.7}^{\text{ClO}})$.

The pressure in the absorption cell was measured with a 1000 Torr capacitance manometer. All gases were mixed prior to entering the photolysis absorption cell. The mass flow rates of the gases and gas mixtures were measured using calibrated mass flow meters. The linear flow velocity of the gases in the absorption cell was normally 10 cm s⁻¹; residence time of the gases in the reaction was 10 s. However, the residence time was varied between 5 and 30 s to test for any changes in σ with this parameter. The photolysis laser was normally operated at ~ 0.1 Hz to ensure that the gas mixture in the absorption cell was completely replenished between laser shots.

Diode Array Spectrum Measurements. Single Absorption Cell Measurements. This apparatus was used to measure the absorption spectrum of NO₃ over the wavelength range 440–720 nm between 298 and 220 K. The absorption spectra were placed on an absolute scale using the absolute absorption cross sections measured at 662 nm as a function of temperature in the pulsed photolysis measurements. The experimental apparatus and methods of data analysis used in these measurements have been described previously¹⁶ and are briefly outlined below.

The apparatus consisted of a light source, a 50-mm-i.d. Pyrex absorption cell with a path length of 200 ± 1 cm, a 0.5-m spectrograph, and a diode array detector. A quartz-halogen lamp (150 W) was operated at low power, to obtain a stable spectral output, and covered the entire wavelength region of this study. The absorption cell was temperature regulated by flowing a cooling fluid through its outer jacket. The temperature over the length of the absorption cell was constant to ± 1 K for temperatures above 240 K but had a 3 K gradient at 220 K. The pressure was measured using 10 and 1000 Torr capacitance manometers. All absorption spectra were measured under flow conditions such that the residence time in the absorption cell was ~ 10 s. Since we are interested only in the shape of the absorption spectrum, any loss of NO₃ as a function of time does not affect our results.

The spectrograph was equipped with a 600 grooves/mm grating and a 1024 element diode array detector. A 150 μm entrance slit, which yielded an instrumental resolution of ~ 0.2 nm, was used for all measurements. Wavelengths were calibrated by using emission lines from Hg, Zn, Cd, and Ne lamps and a 10 μm entrance slit. The wavelength calibration was accurate to ± 0.1 nm. Spectral measurements were made in 84 nm wide segments, the bandwidth of the spectrograph, with a ~ 20 nm overlap between adjacent segments. The shape of the spectra measured in the overlapping wavelength regions agreed within 1% and were averaged in the final analysis. Combinations of long- and short-wavelength cutoff optical filters were mounted in front of the entrance slit of the spectrograph

to minimize the scattered light and eliminate higher order radiation from reaching the detector.

NO₃ was produced at 298 K by the reaction of F with HNO₃ ($k_{298} = 2.3 \times 10^{-11} \text{ cm}^3 \text{ molecule}^{-1} \text{ s}^{-1}$)¹⁵ in a sidearm of the absorption cell:



F atoms were produced in a microwave discharge of a mixture of 5% CF₄ or 10% F₂ in He. A large excess of HNO₃ was used to quickly drive reaction 6 to completion and, hence, minimize the reaction between NO₃ and F atoms. Absorption spectra were recorded using the following procedure. The unattenuated light level, $I_0(\lambda)$, passing through the absorption cell was measured with the microwave discharge turned off but with HNO₃ and CF₄ flowing through the system. Then, the microwave discharge was turned on without changing any of the gas flow rates, which resulted in the production of NO₃. The attenuated light passing through the cell, $I(\lambda)$, was recorded. Spectra were measured in 500 coadded scans. Exposure times varied between 0.028 and 0.12 s, depending on the light intensity, which changed with the wavelength range of the measurement. Each measurement for a given wavelength range and temperature was repeated a minimum of three times and averaged in the final analysis. Absorption spectra at each temperature were calculated using the relation

$$A(\lambda, T) = -\ln[I(\lambda, T)/I_0(\lambda, T)] \quad (\text{VII})$$

Absorption spectra were measured at 298, 280, 260, 240, and 220 K.

The accuracy in the measured NO₃ absorption spectra and their temperature dependence can be estimated from the ratio of the absorption signal, at the various wavelengths, to the stability of the apparatus. With the typical concentrations of NO₃ produced here ($[\text{NO}_3] \sim 1.3 \times 10^{14} \text{ molecules cm}^{-3}$), the absorbance at 662 nm was ~ 0.5 . The fluctuations in the lamp intensity was equivalent to an absorbance of $A = 5 \times 10^{-4}$. Therefore only at the shortest wavelengths, where the absorption cross sections were $< 10^{-19} \text{ cm}^2$, did the apparatus instability contribute to the uncertainty of the measurements.

Another possible source of uncertainty in determining the absorption spectrum is the presence of NO₂ impurities which can result in spectral interferences at the shorter wavelengths where the NO₃ absorption cross sections are small. At 440 nm, the shortest wavelength reported in this study, the NO₃ absorption cross section⁸, is $\sim 2 \times 10^{-19} \text{ cm}^2$ while that of NO₂ is $\sim 5 \times 10^{-19} \text{ cm}^2$.¹⁵ Therefore, small levels of NO₂ impurity will make significant contributions to the measured spectrum. NO₂ could be present either as an impurity in the HNO₃ or formed in the source by the reaction



Absorption spectra of our HNO₃ sample showed that the NO₂ impurity level was less than 100 ppmv. Therefore the NO₂ from the HNO₃ sample would not contribute to the measured NO₃ absorption spectrum. Reference NO₂ absorption spectra were recorded at the same temperature and total pressure used in the NO₃ measurements to estimate NO₂ in the reaction mixture. The diffuse structure in the NO₂ spectrum was used to determine if it contributed to the measured spectrum. Under all conditions, the NO₂ contribution was below the detectable level. Hence, no corrections were necessary.

Dual Absorption Cell Measurements. In addition to the above determinations which utilized one absorption cell, a few measurements were made using a dual absorption cell setup. Here, two 35 cm long absorption cells were connected in series.

One of the cells was cooled to 220 K, and the second cell was held at 298 K. NO₃ was generated in a discharge flow system as described earlier. Both reactions 3 and 6 were used as NO₃ sources. The observed results were independent of the NO₃ source. The spectrograph and the light source were the same as in the single-cell arrangement. The details of the procedures used in such a dual-cell arrangement is given elsewhere.¹⁶ These measurements were not intended to yield quantitative temperature dependent cross section data but only to semiquantitatively check whether the NO₃ absorption cross sections change with temperature. NO₃ was produced in a side arm and flowed first through the 298 K cell and then through the cold cell. Absorptions in both cells were measured using the procedure described by Burkholder et al.¹⁶ The NO₃ formation reaction was run to completion in the sidearm. These measurements of NO₃ absorption at the different temperatures are not quantitative because NO₃ is lost in both of the absorption cells. However, the concentration of NO₃ in the low-temperature cell, the second cell, could only be less than $(298/T_{\text{low}})[\text{NO}_3]_{298}$ where $[\text{NO}_3]_{298}$ is the NO₃ concentration in the first cell. The loss rate of NO₃ was roughly estimated in experiments where both cells were maintained at 298 K by observing the decrease in the NO₃ signal between the two cells; this loss was $\sim 5\text{--}10\%$, which led to an estimated first-order loss rate coefficient of $\sim 0.5 \text{ s}^{-1}$.

The pressure in the flow cells was measured using a 10 Torr capacitance manometer. The gas flow rates were measured using calibrated mass flow meters. The linear flow velocities used in the absorption spectrum measurements were in the range 600–1000 cm s⁻¹. Under these flow conditions there was no measured pressure drop between the two absorption cells.

Materials: ClONO₂ was synthesized by the reaction of Cl₂O with N₂O₅¹⁷ and stored in the dark at 195 K. It was introduced into the absorption cell with a flow of He, which had been passed through a molecular sieve trap at 77 K. The only impurity, detectable by UV absorption, in our ClONO₂ sample was OClO at $\leq 0.006\%$ level. The NO₂ impurity level was estimated to be $< 0.06\%$. O₃ prepared with a commercial ozonizer was stored on silica gel at 195 K and introduced to the absorption cell with a flow of N₂. N₂ (UHP, 99.9995%) was used as supplied. HNO₃ was prepared by mixing KNO₃ with concentrated H₂SO₄ under vacuum and collecting it as a solid in a trap at dry ice temperature. NO₂ was prepared by reacting purified NO with excess O₂ which had been passed through molecular sieve at dry ice temperature. The NO₂ was collected in a dry ice cooled trap and purified by trap-to-trap distillation in an excess O₂ flow until a pure white solid remained.

Results and Discussion

Figure 1 shows typical temporal profiles of the measured absorbances at 253.7 nm in a Cl₂/O₃ mixture and in a Cl₂/ClONO₂ mixture at 662 nm following laser photolysis. The 253.7 nm profiles were measured as part of the actinometry experiments to calibrate the laser fluence. The 662 nm profile was measured after replacing O₃ with ClONO₂ while holding the Cl₂ concentration constant.

The reaction of Cl atoms with O₃ to produce ClO was $> 99\%$ complete within 0.5 ms. At early times following the photolysis laser pulse, the 253.7 nm temporal profile should show the occurrence of this reaction. However, because of the scattered light from the photolysis laser reaching the detector, meaningful absorbances at times less than $\sim 200 \mu\text{s}$ were not possible. The measured absorbance at this wavelength has more scatter than at 662 nm, where the laser intensity is very high and stable. The light intensity at 253.7 nm, the peak of the O₃ absorption,

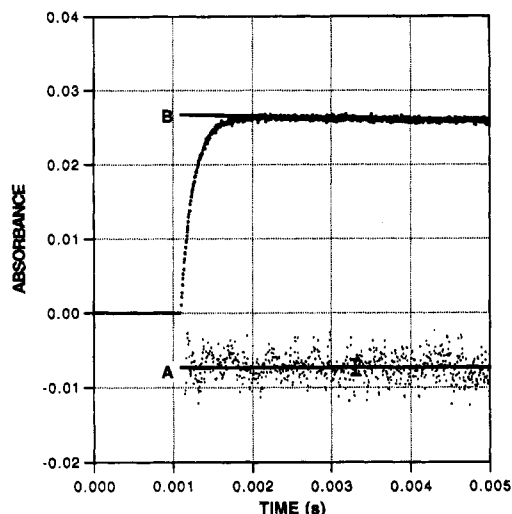


Figure 1. Typical temporal absorption profiles for the laser fluence calibration measurement at 253.7 nm and the standard deviation of the mean absorption value (this deviation has been multiplied by 20 to make it easily visible) (A) and the corresponding NO_3 absorption signal (B) measured following Cl_2 photolysis in the presence of ClONO_2 at 258 K.

was rather low. This is due to the low intensity of the D_2 lamp and the absorption by O_3 . Yet, as seen in Figure 1, the average absorbance measured ~ 0.5 ms after the laser pulse was extremely precise. The average value could be reproduced within a few percent. Figure 1 shows the average value and the standard deviation of the mean of measured absorbance in the plateau region. It should be noted that measurements made with reduced O_3 concentrations, i.e., where the first-order rate coefficient for reaction 2 was smaller, did show a slow decrease in absorption signal at short times consistent with the rate of reaction 4.

The 662 nm temporal profile obtained after the reaction had gone to completion, i.e., 2 ms, was extrapolated to time zero to obtain the absorbance corresponding to the initial concentration of NO_3 , i.e., A_0 . The solid line in Figure 1 is a fit to the slowly decaying NO_3 absorption signal at times greater than 2 ms.

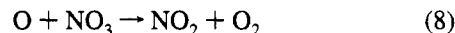
The NO_3 absorption cross section is simply given by the ratio of the maximum absorption signals and the difference in absorption cross sections of O_3 and ClO , according to eq VI. The obtained cross sections and the parameters used in the measurements are given in Table 1. The data used in the determination of the absorption cross section at 298 K are labeled with an asterisk and were measured with a $[\text{ClONO}_2]/[\text{Cl}]_0$ ratio greater than 34. The values of the cross sections measured with $[\text{ClONO}_2]/[\text{Cl}]_0$ ratios less than 34 are also given in the table to illustrate that the amount of NO_3 produced decreases at lower ratios. At the lower values of this ratio, reaction 5 competes with the NO_3 formation via reaction 3 such that $[\text{Cl}]_0$ does not equal $[\text{NO}_3]_{\text{final}}$. If we still assume that $[\text{Cl}]_0 = [\text{NO}_3]_{\infty}$, the absorption cross sections calculated from these measurements decrease systematically as the $[\text{ClONO}_2]/[\text{Cl}]_0$ ratio decreases. At all other temperatures, the $[\text{ClONO}_2]/[\text{Cl}]_0$ ratio greater than 41 were used to avoid this problem.

The 662 nm temporal profile of NO_3 clearly reflects the loss of Cl atoms via its reaction with ClONO_2 . The rate of NO_3 rise was analyzed¹² to obtain the rate coefficient for the loss of Cl. This value agrees very well with the rate coefficient for reaction 3 measured by observing the removal of Cl atoms in an excess of ClONO_2 .¹⁵ As seen in Figure 1, the concentration of NO_3 is zero right after the photolysis laser fires and implies that no significant amount of NO_3 is produced by the photolysis of ClONO_2 . The agreement of the measured rate coefficient for reaction 3 and the lack of initial NO_3 clearly show that the

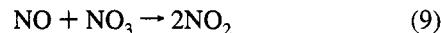
only significant source of NO_3 in this photolysis system was reaction 3. Further, the loss rate of Cl in the absence of ClONO_2 was very small, as shown by the intercept in the plot of the first-order rate coefficient for the appearance of NO_3 versus $[\text{ClONO}_2]$. Therefore, it is clear that essentially all the Cl atoms produced here react with ClONO_2 . If it is assumed that the sole products of this reaction are Cl_2 and NO_3 , the concentration of NO_3 produced must equal that of initially produced Cl atoms.

The average of nine NO_3 absorption cross section measurements at 298 K (weighted by the signal to noise of the measurement) was $(2.23 \pm 0.22) \times 10^{-17} \text{ cm}^2$ (2σ error limits including estimated systematic errors). This value is in excellent agreement with that reported by Sander,⁹ who used methods similar to those used here. Our value is also in excellent agreement with those reported by Canosa-Mas et al.,¹⁸ who used a flow tube with reaction 6 as the source of NO_3 . The absorption cross section reported by Ravishankara and Mauldin¹⁰ is 17% lower than the current measurements. They also used a discharge flow source where NO_3 was produced by reaction 6. Their value barely overlaps with ours within the combined uncertainties of the two measurements.

Sander⁹ has discussed some of the possible problems associated with using a discharge flow system and reaction 6 as the NO_3 source. The basic problem is the loss of NO_3 along the length of the flow tube reactor. If the NO_3 concentration is measured at the entrance of the reactor, the average concentration in the cell would be lower than at the entrance and leads to an underestimation of NO_3 cross section. For example, a first-order rate coefficient for loss of NO_3 of 1 s^{-1} is sufficient to reduce the NO_3 concentration by 5% after 20 cm with a linear flow velocity of $\sim 500 \text{ cm s}^{-1}$ through the cell. Also O atoms generated in the F atom discharge source can reduce the NO_3 concentration through the rapid reaction



where $k_8 = 1 \times 10^{-11} \text{ cm}^3 \text{ molecule}^{-1} \text{ s}^{-1}$ at 298 K.¹⁵ If such complications are occurring, the discharge flow system could yield lower NO_3 absorption cross sections. Canosa-Mas et al.¹⁸ used a discharge flow tube with reaction 6 as the NO_3 source. They point out that the stoichiometry of the titration using reaction with NO



may not be one because of secondary reactions, i.e., $-\Delta[\text{NO}_3] \neq [\text{NO}]_{\text{titration point}}$. After Canosa-Mas et al. corrected for the failure in stoichiometry, they obtained cross sections at 662 nm which are in excellent agreement with the present value. Therefore, there is a possibility that previous measurements, such as that of Ravishankara and Mauldin, which used this titration method may also contain this error. However, correcting the measured titration end points, i.e., concentrations, for the stoichiometry only increases the calculated NO_3 concentrations and hence decreases the calculated absorption cross section. Therefore, the lower values in previous measurements can not be reconciled in this way.

Even though we can not comment on many of the previous measurements, we can note a few points about the studies of Ravishankara and Wine¹⁹ and of Ravishankara and Mauldin.¹⁰ The apparatus used by Ravishankara and Mauldin was essentially identical to that used in their previous 298 K study. In that study, they checked for any significant loss of NO_3 via wall reaction, possible production of O atoms, and production of NO_2 and concluded that they all amounted to an uncertainty of $\sim 13\%$. One observation that could indicate some difficulty in those measurements is that the concentration of NO_2 produced

TABLE 1: Summary of NO₃ Absorption Cross-Section Measurements^a

<i>T</i> (K)	10 ¹⁴ [O ₃]	10 ¹⁶ [Cl ₂]	Δ <i>A</i> _{253.7}	10 ¹³ [Cl] ₀	10 ¹⁴ [ClONO ₂]	[ClONO ₂]/[Cl] ₀	Δ <i>A</i> ₆₆₂	10 ⁻¹⁷ (cm ²) σ ₆₆₂
298	6.37	4.97	0.0169	2.46	6.87	27.9	0.0472	2.11
	6.11	3.88	0.0135	1.96	7.12	36.4	0.0402	2.25 ^b
	5.14	3.53	0.0104	1.51	5.64	34.1	0.0287	2.09 ^b
	4.23	4.03	0.0106	1.53	5.57	36.3	0.0302	2.16 ^b
	4.16	4.04	0.0080	1.17	5.55	47.4	0.0224	2.10 ^b
	4.16	4.04	0.0075	1.08	5.53	51.2	0.0224	2.27 ^b
	3.88	4.07	0.0012	1.74	5.50	315.6	0.00309	1.94 ^b
	3.88	4.07	0.00132	1.92	5.52	287.4	0.00382	2.19 ^b
	6.05	3.06	0.00512	0.744	8.37	112.5	0.0155	2.29 ^b
	5.72	4.07	0.0256	3.73	5.30	14.2	0.0594	1.75
	5.72	4.07	0.0184	2.67	5.31	19.9	0.0480	1.98
	2.51	3.57	0.00946	1.37	9.35	68.0	0.0285	2.28 ^b
	4.27	3.58	0.109	15.9	6.09	3.83	0.133	0.92
	4.27	3.58	0.0891	13.0	6.11	4.70	0.123	1.04
	2.64	3.93	0.0186	2.70	3.21	11.9	0.0404	1.64
							av	2.23 ± 0.09
258	4.89	4.48	0.00494	0.719	4.68	64.9	0.0174	2.66
	4.89	4.48	0.00540	0.784	4.91	59.6	0.0169	2.36
	4.83	4.49	0.00757	1.10	4.69	42.6	0.0260	2.60
	4.83	4.49	0.00787	1.14	4.67	41.0	0.0247	2.37
	2.55	4.04	0.00619	0.900	4.68	52.0	0.0202	2.47
							av	2.49 ± 0.13
230	5.36	5.05	0.00761	1.11	5.12	46.2	0.0282	2.80
	5.36	5.05	0.00732	1.064	5.12	48.1	0.0265	2.74
	5.27	4.42	0.00692	1.01	4.934	49.0	0.0241	2.64
	5.27	4.42	0.00567	0.824	4.94	59.9	0.0214	2.87
							av	2.76 ± 0.13
200	5.86	5.08	0.00616	0.895	5.79	64.7	0.0245	3.01
	5.86	5.08	0.00683	0.992	5.78	58.3	0.0272	3.01
	2.91	4.12	0.00700	1.02	6.05	59.3	0.0284	3.06
	2.91	4.12	0.00636	0.924	6.04	65.4	0.0243	2.89
							av	2.99 ± 0.14

^a Concentrations are in units of cm³ molecule.⁻¹ Quoted uncertainties are 1σ of the measurements. ^b Data used in weighted average.

upon titration with NO was more than that expected from reaction 9. However, their NO₂ concentration in the absence of NO was not very large, <40% of [NO₃]. Therefore, we cannot definitively say that either the secondary reactions or errors in stoichiometry of the titration are the source of the discrepancy in that study. Yet, since the current work has the benefit of all the findings to date, it supersedes the results presented by Ravishankara and Mauldin.

The room-temperature value of Cantrell et al.,⁸ 2.08 × 10⁻¹⁷ cm², is also in good agreement with our value and that of Sander.⁹

We measure a monotonic increase in the NO₃ absorption cross section at 662 nm with decreasing temperature. The absorption cross section increased by 35% in going from 298 to 200 K. A comparison of our results with those of Sander,⁹ Ravishankara and Mauldin,¹⁰ and Cantrell et al.⁸ is given in Figure 2. The agreement between our measurements and those of Sander⁹ is excellent. The temperature dependence seen by Ravishankara and Mauldin is also similar, though they see a slightly larger variation. Even though the 2σ error limits for the two studies do overlap, our measured trend in cross sections with temperature does not agree with that reported by Cantrell et al.⁸ Over the temperature range 348–215 K, they find the NO₃ absorption cross section at 661.9 nm to be independent of temperature.

We also estimated the temperature dependence of the NO₃ absorption cross section at 662 nm using two absorption cells connected in series. In these experiments, NO₃ flowed from the warm cell to the cold cell. After accounting for the change in number density with temperature we could clearly see a 15% increase in the absorption at 662 nm, even when we assumed that there was no loss of NO₃ in either cells. If we account for the loss of NO₃ in flowing from one cell to another, the observed change in absorption agreed extremely well with that measured using the single cell. At 220 K the cross section was 30% higher than at 298 K, while the single cell arrangement gave a 28%

increase for the same change in temperature. These measurements unambiguously show that the cross section increases with decreases in temperature.

The reason for the discrepancy between our measurements and those of Cantrell et al. are not clear. However, it should be noted that Cantrell et al. used an indirect method for determining the NO₃ concentration. It is possible that wall loss of N₂O₅ in their experiments to generate HNO₃ could account for some of the discrepancies. A wall loss would cause errors in their gas-phase NO₃ abundance and mass balance. The wall loss rate could change with temperature and mask the change in NO₃ absorption cross section with temperature. Cantrell et al. acknowledged that such a loss would lead to errors in their measurements, but discounted the possibility. Some measurements in our laboratory have shown that uptake of N₂O₅ on cold glass is reasonably efficient, i.e., γ = 0.001, and if there is any ice it increases²⁰ to ~0.1. Therefore, it is not clear if surface uptake was avoided in the measurements of Cantrell et al. Last, Cantrell et al. used very large NO₃ absorbances, often greater than 10. At such low levels of light transmission the absorbance values are very dependent on the baseline stability of the measurement apparatus. It is not clear, however, how this would affect the accuracy of the calculated absorption cross sections.

As mentioned in the Experimental Section, we also measured the NO₃ absorption spectrum using a diode array spectrometer as a function of temperature. The room-temperature absorption spectrum is shown in Figure 3 normalized to the absorption cross section determined in the laser photolysis experiments. The inset in Figure 3 shows the temperature dependence of the 0–0 band at 298, 280, 260, 240, and 220 K, where again the absorption cross sections are taken from the photolysis measurements. The peak cross sections at these temperatures were obtained from a linear interpolation of the cross sections measured using the photolysis system at various temperatures,

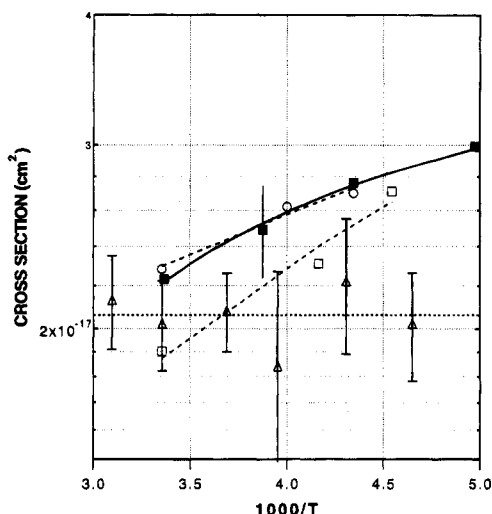


Figure 2. Comparison of the 662 nm temperature-dependent NO_3 cross-section measurements: this work (solid squares and curve), Sander⁹ (open circles and dashed line), Ravishankara and Mauldin²¹ (open squares and dashed line), and Cantrell et al.⁸ (open triangles and dashed line).

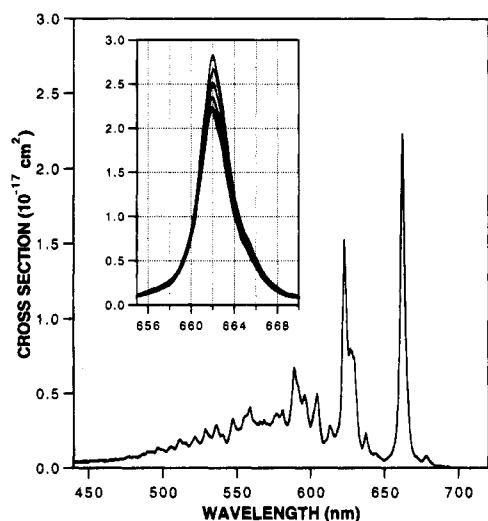


Figure 3. NO_3 absorption spectrum at 298 K. The inset figure shows the temperature dependence of the 0–0 band in going from 298 K (lowest peak cross section) to 220 K (highest peak cross section). The intermediate spectra are at $T = 280, 260,$ and 240 K.

$\sigma_{661.9} = (4.56 - 0.00787T) \times 10^{-17} \text{ cm}^2$. Our spectrum is in good agreement with those reported previously at 298 K.⁷ The changes in cross sections at wavelengths shorter than 610 nm are slightly smaller than that observed at the peak.

The structure in the NO_3 absorption spectrum showed small but systematic dependencies on the temperature. The largest changes were observed in the relative peak heights of the 662 nm and 623 nm bands. Also the relative height of the 623 nm peak to the shoulder at 628 nm shows a dependence on temperature. The ratio of the absorption at 662 nm to that at 623 nm at 298 K is 1.47 in our spectrum. This ratio is 1.42 in the data reported by Sander.⁹ This ratio increases to 1.51 at 220 K. Sander⁹ also observed such an increase in this ratio with decreasing temperature; the value was 1.53 at 230 K, in good agreement with our results. Cantrell et al.⁸ do not report digitized spectral data. However, their Figure 3 shows an absorption spectrum recorded at 215 K. Taking the peak signals from this figure gives a ratio of 1.63 at 215 K. This value is

significantly higher than those measured by us and Sander. Therefore it appears that our results disagree with those of Cantrell et al.⁸ on the magnitude of the change in absorption cross section with temperature and the shape of the spectrum as a function of temperature. Note that the ratio of the cross sections at two wavelengths do not depend on the absolute cross sections and can be very accurately determined.

Atmospheric Implications. Our results, in conjunction with previous results, show that the absorption cross section at 662 nm for atmospheric measurements would be $2.23 \times 10^{-17} \text{ cm}^2$ at 298 K, and it increases with decreasing temperatures. The atmospheric photolysis rate of NO_3 is not very sensitive to the changes in temperature because the cross sections do not change very much in the wavelength regions where absorption leads to dissociation. Previously, Ravishankara et al.²¹ have measured the rate coefficient for the $\text{OH} + \text{HNO}_3$ reaction, as well as the yield of NO_3 , by monitoring NO_3 absorption at 662 nm. Any changes in the absorption cross sections do not, of course, affect the rate coefficient data. However, if we use the cross section at 662 nm measured here, the yield of NO_3 derived in those measurements decreases from 0.98 to 0.85 at 298 K and from 1.17 to 0.88 at 251 K. The difference in the yields measured at 298 and 251 K appear to be entirely due to the increases in the cross sections of NO_3 with decreasing temperatures.

Acknowledgment. This work was supported in part by the National Aeronautics and Space Administration Upper Atmosphere Research Program.

References and Notes

- Solomon, S.; Miller, H. L.; Smith, J. P.; Sanders, R. W.; Mount, G. H.; Schmeltekopf, A. L.; Noxon, J. F. *J. Geophys. Res.* **1989**, *94*, 11041.
- Noxon, J. F.; Norton, R. B.; Henderson, W. R. *Geophys. Res. Lett.* **1978**, *5*, 675.
- Noxon, J. F.; Norton, R. B.; Marovich, E. *Geophys. Res. Lett.* **1980**, *7*, 125.
- Noxon, J. F. *J. Geophys. Res.* **1983**, *88*, 11017.
- Platt, U.; Perner, D.; Schroeder, J.; Kessler, C.; Toenissen, A. *J. Geophys. Res.* **1981**, *86*, 11965.
- Platt, U.; Perner, D.; Winer, A. M.; Harris, G. W.; Pitts, J. N. *Geophys. Res. Lett.* **1980**, *7*, 89.
- Wayne, R. P.; Barnes, I.; Biggs, P.; Burrows, J. P.; Canosa-Mas, C. E.; Hjorth, J.; Lebras, G.; Moortgat, G. K.; Perner, D.; Poulet, G.; Restelli, G.; Sidebottom, H. *Atmos. Environ.* **1991**, *25*, 1.
- Cantrell, C. A.; Davidson, J. A.; Shetter, R. E.; Anderson, B. A.; Calvert, J. G. *J. Phys. Chem.* **1987**, *91*, 5858.
- Sander, S. P. *J. Phys. Chem.* **1986**, *90*, 4135.
- Ravishankara, A. R.; Mauldin, III, R. L. *J. Geophys. Res.* **1986**, *91*, 8709.
- Yokelson, R. L.; Burkholder, J. B.; Ravishankara, A. R., manuscript in preparation.
- Yokelson, R. L.; Burkholder, J. B.; Fox, R. W.; Goldfarb, L.; Gilles, M. K.; Ravishankara, A. R. *J. Chem. Kinetics*, manuscript in preparation.
- Burkholder, J. B.; Mauldin, R. L., III; Yokelson, R. L.; Solomon, S.; Ravishankara, A. R. *J. Phys. Chem.* **1993**, *97*, 7597.
- Mauldin, R. L., III; Burkholder, J. B.; Ravishankara, A. R. *J. Phys. Chem.* **1992**, *96*, 2582.
- DeMore, W. B.; Sander, S. P.; Golden, D. M.; Hampson, R. F.; Kurylo, M. J.; Howard, C. J.; Ravishankara, A. R.; Kolb, C. E.; Molina, M. J. *Chemical Kinetics and Photochemical Data for use in Stratospheric Modeling*; Jet Propulsion Laboratory, JPL Pub. No. 92-20, 1992.
- Burkholder, J. B.; Talukdar, R. K.; Ravishankara, A. R.; Solomon, S. *J. Geophys. Res.* **1993**, *98*, 22937.
- Burkholder, J. B.; Talukdar, R. K.; Ravishankara, A. R. *Geophys. Res. Lett.* **1993**, *21*, 585.
- Canosa-Mas, C. E.; Fowles, M.; Houghton, P. J.; Wayne, R. P. *J. Chem. Soc., Faraday Trans. 2* **1987**, *83*, 1465.
- Ravishankara, A. R.; Wine, P. H. *Chem. Phys. Lett.* **1983**, *101*, 73.
- Hanson, D. R.; Ravishankara, A. R. *J. Phys. Chem.* **1993**, *97*, 2802.
- Ravishankara, A. R.; Eisele, F. L.; Wine, P. H. *J. Phys. Chem.* **1982**, *86*, 1854.